

## LEED-IV study of the rutile $\text{TiO}_2(110)-1 \times 2$ surface with a Ti-interstitial added-row reconstruction

M. Blanco-Rey,<sup>1,\*</sup> J. Abad,<sup>2</sup> C. Rogero,<sup>3</sup> J. Méndez,<sup>1</sup> M. F. López,<sup>1</sup> E. Román,<sup>1</sup> J. A. Martín-Gago,<sup>1</sup> and P. L. de Andrés<sup>1</sup>

<sup>1</sup>*Instituto de Ciencia de Materiales (CSIC), Cantoblanco, 28049 Madrid, Spain*

<sup>2</sup>*Centro de Investigación en Óptica y Nanofísica, Universidad de Murcia, Campus Espinardo, 30100 Murcia, Spain*

<sup>3</sup>*Centro de Astrobiología (CSIC-INTA), Carretera de Ajalvir km. 4, 28850 Torrejón de Ardoz, Madrid, Spain*

(Received 22 November 2006; revised manuscript received 22 December 2006; published 9 February 2007)

Upon sputtering and annealing in UHV at  $\sim 1000$  K, the rutile  $\text{TiO}_2(110)$  surface undergoes a  $1 \times 1 \rightarrow 1 \times 2$  phase transition. The resulting  $1 \times 2$  surface is Ti rich, formed by strands of double Ti rows as seen on scanning tunneling microscopic images, but its detailed structure and composition have been subject to debate in the literature for years. Recently, Park *et al.* [Phys. Rev. Lett. **96**, 226105 (2006)] have proposed a model where Ti atoms are located on interstitial sites with  $\text{Ti}_2\text{O}$  stoichiometry. This model, when it is analyzed using LEED-IV data [Phys. Rev. Lett. **96**, 0055502 (2006)], does not yield an agreement between theory and experiment as good as the previous best fit for Onishi and Iwasawa's model for the long-range  $1 \times 2$  reconstruction. Therefore, the  $\text{Ti}_2\text{O}_3$  added row is the preferred one from the point of view low-energy electron diffraction.

DOI: [10.1103/PhysRevB.75.081402](https://doi.org/10.1103/PhysRevB.75.081402)

PACS number(s): 61.14.Hg, 68.35.Bs, 68.47.Gh

Metal oxide surfaces are a subject of strategic interest due to their wide range of technological applications. They are popular as a support for heterogeneous catalysis, but are also highly appreciated for their use in photocatalysis, anticorrosion coatings, pigments, gas sensing, biocompatibility, environmental applications, etc.<sup>1</sup> Among the different rutile surfaces,  $\text{TiO}_2(110)$  is the most popular due to its stability and favorable morphology, and it is considered in the literature as a benchmark for modeling the structure and electronic properties of metal oxides. The bulk rutile is characterized by rows of alternatively oriented oxygen octahedra centered at titanium atoms. The  $\{110\}$  cut produces a relatively flat surface; however, only recently has a structural determination by low-energy electron diffraction (LEED) been considered accurate enough to bring wide consensus to the quantitative values for the different atomic positions.<sup>2</sup> Most interesting, moreover, is the  $1 \times 2$  reconstruction that appears on the clean surface upon annealing up to  $\sim 1000$  K in ultrahigh vacuum (UHV). From scanning tunneling microscopy (STM) it has been well established that this phase consists of long stripes running along the  $[001]$  crystallographic direction. By careful formation of this new stable phase, these chains can be formed nearly without interruption on the typical distances of terraces—i.e., 100–1000 Å long. These chains are known to depart from the surface stoichiometry and are usually characterized as a reduced Ti rich  $1 \times 2$  reconstruction.<sup>3</sup> From a combined approach using STM, LEED and density functional theory (DFT), recently we predicted that these stripes may possess interesting quasi-one-dimensional properties.<sup>4</sup> The complexity of the reconstruction, however, is enough to allow for many different geometrical configurations; even a possible reversible transformation between the  $1 \times 1$  and the  $1 \times 2$  phases has been reported,<sup>5</sup> not to mention the existence of *cross-links* between chains with an entirely different stoichiometry or other defects on the surface.<sup>6</sup> Some of these phenomena might well depend on the careful conditions to recreate the  $1 \times 2$  reconstruction, and the fact is that this system is a challenge

for both theory and experiment. Therefore, it is important to realize that the formation of a  $1 \times 2$  phase may certainly be influenced by external parameters (e.g., UHV or not, the particular ambience if any, different temperatures and times for annealing, etc). The geometrical structure of the  $1 \times 2$  phase has been much studied in the literature by STM, but these experiments cannot give a clear description of the atomic positions or even the surface stoichiometry. Hence, different proposals can be found in the literature: (i) a missing-row model<sup>7</sup> where bridging oxygen atoms are desorbed into vacuum in competition with diffusion of bulk lattice oxygen atoms moving to the surface, (ii) an added-row model with a  $\text{Ti}_2\text{O}_3$  stoichiometry<sup>3</sup> where the Ti cations move to octahedral sites and oxygen atoms stay near their bulklike positions, (iii) an added-row model with a  $\text{Ti}_3\text{O}_5$  stoichiometry<sup>8</sup> where all the atoms remain near their bulk positions, and (iv) a stoichiometric model<sup>6</sup> where the added rows proposed by Pang *et al.* have been modified by adding oxygen to create an added row of  $\text{Ti}_3\text{O}_6$ .

LEED is known to be very sensitive to the final disposition of the atoms on the surface. However, by analyzing only the Bragg spots, we obtain information about the ordered long-range structures. To study the geometry of disordered short-range structures, defects, etc. one should focus on the diffuse LEED intensities measured at low-temperatures, which is beyond our experimental setup. We have used LEED-IV for the  $1 \times 2$  reconstruction to test all these different models against full multiple-scattering calculations.<sup>4</sup> An objective quantitative comparison between experimental and theoretical LEED-IV curves can be obtained by computing a suitable  $R$  factor that can be used to identify relevant best-fit models. We have used Pendry's  $R$  factor,<sup>9</sup> a widely accepted relevant and accurate number to characterize real structures.<sup>10</sup> Pendry's  $R$  factor  $R_p$  takes values between 0 and 2; values below 0.3 yield a reasonable good correlation between theory and experiment, while values over 0.5 mark the onset of spurious chaotic correlations.<sup>11</sup>

Recently, a new structural candidate for the  $1 \times 2$  recon-

struction has been put forward by Park *et al.*<sup>12</sup> The model is quite attractive for a number of interesting features; e.g., it provides a natural mechanism to explain the transition between the  $1 \times 1$  and the  $1 \times 2$  phases. This model is based in two observations: (i) half-step terraces in  $1 \times 1$  samples, which have been considered by Park *et al.* as a sign of a change from edge- to face-sharing oxygen octahedra with respect to the lower terrace, and (ii) added TiO strands are linear localized defects observable by high-resolution STM. Upon reduction of an added strand lying by the half-step terrace edge, a precursor of the  $1 \times 2$  structure can be modeled. However, due to the short-range-order character of these defects, it is not obvious how to map this local transition model onto an extended fully ordered  $1 \times 2$  phase. Thus, it is important to test the periodic  $1 \times 2$  model proposed by Park *et al.*, which departs substantially from previous ones in the literature, against as many quantitative experimental observations as possible. The aim of this work is to determine whether this newly proposed structure, and possibly some logical variations compatible with the STM images,<sup>4</sup> fits our previously reported LEED-IV measurements better than the best previous candidate (Onishi-Iwasawa  $\text{Ti}_2\text{O}_3$  model) or not.

Detailed information on the experimental procedure to obtain the  $1 \times 2$  reconstruction has been published elsewhere.<sup>4</sup> Here, we summarize the more relevant steps: a rutile single crystal (PI-KEM Ltd., UK) has been subjected to repeated cycles of 1-keV Ar<sup>+</sup> sputtering and high-temperature annealing (1150 K) under UHV conditions (base pressure  $2 \times 10^{-10}$  mbar). Surface cleanliness has been checked by Auger spectroscopy. A sharp  $1 \times 2$  LEED pattern, with low background, has been observed. Constant-current-mode STM images, recorded *in situ* at room temperature over typical areas of  $100 \text{ \AA}^2$ , show bright long stripes separated by  $13 \pm 1 \text{ \AA}$ , no cross-links, monoatomic steps of  $3.2 \pm 0.2 \text{ \AA}$ , and large terraces more than  $100 \text{ \AA}$  wide.<sup>4</sup> LEED-IV experiments were performed at room temperature by using an 8-bit charge-coupled-device (CCD) camera. Prolonged electron-beam exposure during the LEED-IV measurements produce degradation of the sample as seen in the loss of quality of fractional spots and the increase of background intensity. To avoid these effects, the sample was displaced at short time intervals to expose new fresh areas to the electron beam and the sample was regularly reannealed to restore the LEED pattern to the initial quality.

Two Ti interstitial site types can be found in the rutile bulk structure. The notation used in this paper follows the convention of Ref. 13: in the *ih* site (*iv* site) the Ti atom occupies the center of an octahedra with the equatorial plane parallel (perpendicular) to the surface. The model proposed by Park *et al.*,<sup>12</sup> shown in Fig. 1, consists of added rows of  $\text{Ti}_2\text{O}$  stoichiometry. Strictly speaking, interstitials are meaningless on the surface, but we follow the standard notation already spread in the literature and use the word for Ti(*a*) atoms. In this model, Ti(*a*) atoms occupy *ih* sites; i.e., they lie on atop the position with respect to the underlying threefold-coordinated O(4). We remark that the previously accepted Onishi-Iwasawa model<sup>3,4</sup> involves *iv* sites, a situation where Ti(*a*) lies on bridge position with respect to O(4) atoms. These Ti(*a*) atoms with formal charge 3+ are exposed

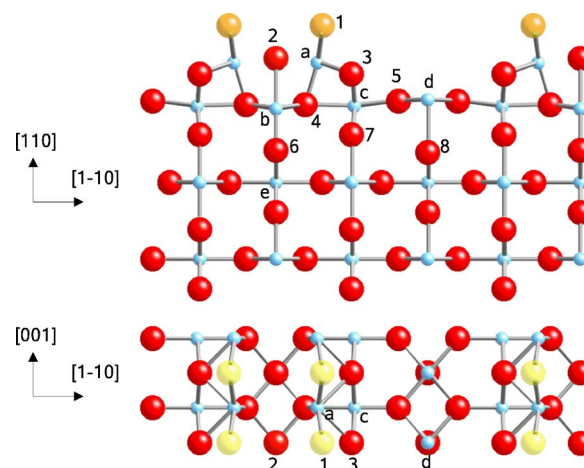


FIG. 1. (Color online) Side and top views of the ball and stick model for the double-strand  $\text{TiO}(110)\text{-}1 \times 2$  surface according to Park *et al.* (Ref. 12) with  $\text{Ti}(\text{ih})_2\text{O}$ . Small (blue) balls (labeled by letters) represent Ti atoms, while large (red) balls (labeled by numbers) are O atoms. In the top view only top layer and reconstruction atoms are shown. Atomic positions have been allowed to relax to maximize the correlation between calculated LEED-IV curves for those models and the experimental ones. The best experiment-theory fit results in a Pendry  $R$  factor  $R_p=0.45$ . The addition of O(1) rows [large yellow (light gray) balls] results in the  $\text{Ti}(\text{ih})_2\text{O}_3$  structure discussed in the text.

in the model of Park *et al.*, while in the Onishi-Iwasawa model a the bridging O row atom is adsorbed on top of the  $\text{Ti}^{3+}$ . Therefore, we further test Park's *et al.* by considering a simple variation: an O-terminated one.

An STM study alone cannot distinguish the stoichiometry of the added rows, neither could it discriminate between the *ih* site or *iv* site for Ti(*a*).<sup>4</sup> DFT alone could in principle determine the right structure, but the great complexity of the parameter space makes this a daunting task if DFT is not supplemented with external structural information. Indeed, DFT calculations rely on some approximations (e.g., they usually assume  $T=0 \text{ K}$ , strong correlation is not well described, etc.), which makes it desirable to complement this kind of approach with a different technique directly related to the structure. We have used quantitative LEED-IV to decide whether the  $\text{Ti}(\text{ih})_2\text{O}$  model proposed by Park *et al.* fits well with our experimental database on this surface. The spectra database contains integer and half-integer diffraction beams. For this work, we have only used the portion of the data taken under normal-incidence conditions, as it seems large enough to reach an accurate conclusion. The total energy overlap between experiment and theory (a measure of the size of the database and then related to the accuracy in the determination) has been  $\Delta E=1424 \text{ eV}$ . Finally,  $I(V)$  curves have been symmetry averaged to improve the signal-to-noise ratio.

First, full-dynamical  $I(V)$  evaluations have been done for reference  $\text{Ti}(\text{ih})_2\text{O}$  structures. Here, composite-layer and layer-doubling approaches are used. Afterwards, we applied tensor-LEED theory to efficiently study distortions from our initial reference.<sup>14,15</sup> This part of the structural search has been limited to structures where none of the geometrical pa-

TABLE I. Optimized  $xyz$  positions ( $OZ$  axis points inwards) and thermal vibration amplitudes ( $u$ ) in  $\text{\AA}$  for the  $\text{Ti}(ih)_2\text{O}$  added-row model shown in Fig. 1.

Atom	$x$	$y$	$z$	$u$
Ti( $a$ )	1.57	0.00	$-5.12\pm 0.14$	0.30
Ti( $b$ )	0.00	1.48	$-3.14\pm 0.10$	0.12
Ti( $c$ )	3.32	0.00	$-3.26\pm 0.10$	0.12
Ti( $d$ )	6.49	1.48	$-3.52\pm 0.06$	0.12
O(2)	0.00	1.48	$-5.30\pm 0.12$	0.22
O(3)	3.14	1.48	$-4.63\pm 0.14$	0.14
O(4)	1.26	0.00	$-3.32\pm 0.18$	0.16
O(5)	5.22	0.00	$-3.48\pm 0.16$	0.16
O(6)	0.00	1.48	$-1.38\pm 0.32$	0.10
O(7)	3.24	1.48	$-2.04\pm 0.12$	0.10
O(8)	6.49	1.48	$-1.28\pm 0.20$	0.10

rameters have changed by an amount larger than  $\sim 0.4 \text{\AA}$ , which is a widely accepted validity range for tensor-LEED. Whenever the structure escaped away from the convergence region, a new reference structure was formed and fresh full-dynamical calculations performed again. Comparison between calculated and experimental spectra is made via Pendry's  $R$  factor prescription  $R_p$  (Ref. 9).

In  $\text{TiO}_2$  LEED-IV calculations, phase shifts have been shown to be an important ingredient,<sup>2</sup> although it is now accepted that a full self-consistent calculation does not seem to be necessary. However, the muffin-tin radii must be carefully chosen, with help from *ab initio* electronic structure calculations. A value of  $\sim 1 \text{\AA}$  for both atomic species can be estimated from GAUSSIAN calculations of the charge distribution in a  $\text{TiO}_2$  molecule,<sup>4</sup> which is found to provide satisfactory spectra. For the available energy range, the maximum angular momentum number required is  $l_{\text{max}}=8$ .

Seventeen atoms have been included in the search; relevant parameters include both geometry positions for the atoms and thermal vibration amplitudes. Because the parameter space to be surveyed is large, some restrictions need to be imposed. Lateral movements have been restricted because the LEED normal incidence is quite insensitive to them. Only models consistent with the experimental diffracted intensities symmetry have been considered. The algorithm to search has been the random sampling algorithm (RSA), as implemented in the Erlangen LEED package.<sup>15,16</sup>

Best-fit atomic positions for the  $\text{Ti}(ih)_2\text{O}$  model after the geometrical parameters have been allowed to relax are shown in Fig. 1, and the corresponding coordinates and thermal vibration amplitude values are summarized in Table I. The best  $R$  factor achieved for this  $I(V)$  fit is  $R_p=0.45\pm 0.08$  (see Fig. 2), a value that is not usually considered satisfactory in LEED structural work. Individual beam  $R_p$  values are high, too. Other nonstructural fitted parameters are  $V_{oi}=5.5 \text{ eV}$  and  $V_{or}=8.0 \text{ eV}$  for real and imaginary parts of the self-energy, respectively, which are similar to the previously reported values for the  $\text{Ti}(iv)_2\text{O}_3$  model.<sup>4</sup> The strong damping in the experimental LEED intensities at high energies yields large fitted vibration amplitude values of  $\text{Ti}(ih)_2\text{O}$  group atoms, also shown in Table I.

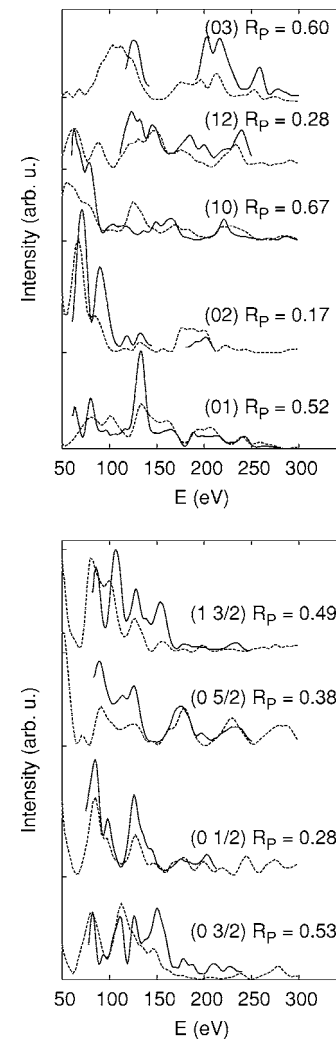


FIG. 2. Experimental  $I(V)$  curves (solid line) and calculated curves (dashed line) for the optimized geometry of Table I.

The obtained structure shows no significant buckling at the five-fold-coordinated Ti( $d$ ) atom, in contrast to the strong one found for  $\text{Ti}(iv)_2\text{O}_3$ , where Ti( $d$ ) relaxed inwards and the difference in the vertical coordinates of Ti( $d$ ) and O(5) was  $0.46 \text{\AA}$ <sup>4</sup> (see Fig. 1).

The vertical distance between the Ti( $a$ ) atom and the trough Ti( $d$ ) atom is  $1.6 \text{\AA}$ , in good agreement with the terrace height found by DFT calculations<sup>12</sup> (see Fig. 1). Ti( $a$ )-O(2) distance is  $2.32 \text{\AA}$ , larger than the  $2.07 \text{\AA}$  value reported by Park *et al.*, since the Ti( $a$ ) atom does not occupy a fully atop position upon O(4) in the LEED-optimized structure. Besides, the bridging O(3) rows are not pulled towards Ti( $a$ ) atoms. In the geometry found by LEED, the bridging O(3) row, parallel to  $[001]$ , deviates from the surface normal by a tilt angle  $7.5^\circ$ , smaller than the  $20^\circ$  angle predicted by DFT.<sup>12</sup> The latter DFT tilt value is in agreement with electron-stimulated desorption ion angular distribution (ESDIAD) experiments which yield a desorption angle of  $18\pm 5^\circ$  for  $\text{O}^+$  ions from the  $1\times 2$  surface.<sup>17</sup>

STM imaging of adsorbed formate ions ( $\text{DCOO}^-$ ) on the  $1\times 2$  surface suggests the absence of exposed Ti ions in the

added rows.<sup>18</sup> Thus, the possibility of a double O row sitting on the strands, while keeping the Ti(*a*) atoms on *ih* sites, has been examined. This is a simple transformation from the one of Park *et al.*, although it was not proposed in Park's original paper. However, no significant improvement has been found. The Ti(*iv*)<sub>2</sub>O<sub>3</sub> model fit yields a satisfactory  $R_p = 0.28 \pm 0.04$  against other models,<sup>4</sup> and removal of topmost O(1) atom from that structure does not cause a significantly worse fit. In fact, a Ti(*iv*)<sub>2</sub>O model can be optimized to  $R_p = 0.32$ . However, the latter result can be interpreted as a consequence of statistical correlations between site occupancies and thermal vibration amplitudes.

Thus, from LEED observations we can conclude that our sample structure has a double strand of Ti atoms occupying *iv* sites rather than *ih* sites. DFT calculations show that Ti(*ih*)<sub>2</sub>O<sub>3</sub> is an unstable structure, which yields the Ti(*iv*)<sub>2</sub>O<sub>3</sub> model upon geometry optimization.<sup>13</sup> LEED seems not to be sensitive enough to topmost O(1) atoms, but it must be borne in mind that, according to the findings of Ref. 18, the exposed Ti models are improbable. ESDIAD results can also be explained by a Ti<sub>2</sub>O<sub>3</sub> model, where topmost O(1) atoms (see Fig. 1) also desorb in an off-normal direction. However, in the Ti(*iv*)<sub>2</sub>O<sub>3</sub> structure determined from LEED-IV,<sup>4</sup> the tilt angles of both O(1) and O(3) atoms, 11° and 9°, respectively, are smaller than the corresponding value from ESDIAD.

The Ti(*ih*)<sub>2</sub>O model shows important differences between LEED and DFT for components of atomic vector positions parallel to the surface. One should keep in mind that normal-incidence LEED is not very accurate for these values. We have started different LEED calculations around reasonable

combinations of parameters suggested by DFT.<sup>19</sup> To make sure that we did not miss a nearby optimum structure, a thorough exploration around all these starting points has been performed with an efficient perturbative approach: namely, tensor-LEED.<sup>14</sup> None of these attempts significantly improved the *R* factor; the chances we might have missed a difficult minimum should be very small.

A word of caution is in order due to the appearance of a cross-linked structure after several annealing cycles. This might be interpreted as an indication of the metastable character of the added-row model.<sup>20</sup> Therefore, the existence of a Ti(*ih*)<sub>2</sub>O<sub>x</sub> structure should not be completely ruled out; it might be part of a metastable state in the transition, which might be reached by the system through a different phase transition mechanism. The particular experimental conditions to reach the surface would in that case be crucial. Furthermore, coexisting equilibrium phases might eventually be found under certain conditions of temperature, atmosphere, gas pressure, bulk defect concentration, etc. Although not likely for our experimental conditions, this cannot be completely ruled out because the description of the phase diagram for TiO<sub>2</sub>(110) is a challenging topic not yet fully completed.<sup>21</sup>

This work has been financed by the CYCIT (Grant No. MAT-2005-3866). M.B.R. acknowledges Spanish CSIC for financial support through I3P program. The Barcelona Supercomputer Center (<http://www.bsc.es/>) is acknowledged for computing time. K. T. Park and R. Lindsay are acknowledged for useful discussions.

\*Present address: Department of Chemistry, University of Cambridge, Lensfield Road, Cambridge CB2 1EW, UK. Electronic address: mb633@cam.ac.uk

<sup>1</sup>U. Diebold, *Surf. Sci. Rep.* **48**, 53 (2003).

<sup>2</sup>R. Lindsay, A. Wander, A. Ernst, B. Montanari, G. Thornton, and N. M. Harrison, *Phys. Rev. Lett.* **94**, 246102 (2005).

<sup>3</sup>H. Onishi and Y. Iwasawa, *Surf. Sci. Lett.* **313**, 783 (1994).

<sup>4</sup>M. Blanco-Rey, J. Abad, C. Rogero, J. Mendez, M. F. Lopez, J. A. Martin-Gago, and P. L. de Andres, *Phys. Rev. Lett.* **96**, 055502 (2006).

<sup>5</sup>K. F. McCarty and N. C. Bartelt, *Phys. Rev. Lett.* **90**, 046104 (2003).

<sup>6</sup>R. A. Bennett, P. Stone, and M. Bowker, *Faraday Discuss.* **114**, 267 (1999).

<sup>7</sup>P. J. Möller and M.-C. Wu, *Surf. Sci.* **224**, 265 (1989).

<sup>8</sup>C. L. Pang, S. A. Haycock, H. Raza, P. W. Murray, G. Thornton, O. Gulseren, R. James, and D. W. Bullett, *Phys. Rev. B* **58**, 1586 (1998).

<sup>9</sup>J. Pendry, *J. Phys. C* **13**, 937 (1980).

<sup>10</sup>P. Watson, M. V. Hove, and K. Hermann, NIST Surface Structure Database V4.0, NIST Standard Reference Data Program, Gaithersburg, MD 2002.

<sup>11</sup>P. L. de Andrés and J. A. Vergés, *Phys. Rev. B* **59**, 3086 (1999).

<sup>12</sup>K. T. Park, M. H. Pan, V. Meunier, and E. W. Plummer, *Phys. Rev. Lett.* **96**, 226105 (2006).

<sup>13</sup>S. D. Elliott and S. P. Bates, *Phys. Rev. B* **65**, 245415 (2002).

<sup>14</sup>P. J. Rous, J. B. Pendry, D. K. Saldin, K. Heinz, K. Müller, and N. Bickel, *Phys. Rev. Lett.* **57**, 2951 (1986).

<sup>15</sup>V. Blum and K. Heinz, *Comput. Phys. Commun.* **134**, 392 (2001).

<sup>16</sup>M. Kottcke and K. Heinz, *Surf. Sci.* **376**, 352 (1977).

<sup>17</sup>Q. Guo, I. Cocks, and E. M. Williams, *Phys. Rev. Lett.* **77**, 3851 (1996).

<sup>18</sup>H. Onishi, K. Fukui, and Y. Iwasawa, *Bull. Chem. Soc. Jpn.* **68**, 2447 (1995).

<sup>19</sup>K. T. Park (private communication).

<sup>20</sup>R. A. Bennett, P. Stone, N. J. Price, and M. Bowker, *Phys. Rev. Lett.* **82**, 3831 (1999).

<sup>21</sup>K. F. McCarty and N. C. Bartelt, *Surf. Sci.* **527**, L203 (2003).